

## Water ingress into starch and sucrose:starch systems

I. Hopkinson<sup>a,\*</sup>, R.A.L. Jones<sup>b</sup>, P.J. McDonald<sup>c</sup>, B. Newling<sup>c</sup>, A. Lecat<sup>d</sup>, S. Livings<sup>e</sup>

<sup>a</sup>*Cavendish Laboratory, Polymers and Colloids Group, University of Cambridge, Cambridge CB3 0HE, UK*

<sup>b</sup>*Department of Physics, University of Sheffield, Sheffield S3 7RH, UK*

<sup>c</sup>*Department of Physics, University of Surrey, Guildford, Surrey GU2 5XH, UK*

<sup>d</sup>*Nestlé Product Technology Centre York, P.O. Box 204, Haxby Road, York YO1 1XY, UK*

<sup>e</sup>*Nestlé R&D, Inc., 201 Housatonic Avenue, New Milford, CT 06776, USA*

Received 21 June 2000; received in revised form 3 November 2000; accepted 5 December 2000

### Abstract

The ingress of water from various solutions into dense starch and sucrose:starch plaques has been observed over a range of temperatures using stray field nuclear magnetic resonance imaging. Profiles of water content as a function of depth from the surface and sorption time have been analysed to obtain mutual diffusion coefficients. This has been done using the Boltzmann transform and by measuring the front position as a function of time which produces an average mutual diffusion coefficient. This average diffusion coefficient can be fit with an Arrhenius expression with an activation energy of  $56 \pm 4 \text{ kJ mol}^{-1}$ . It was found that the average diffusion coefficients for 30:70 and 50:50 sucrose:starch mixtures could be calculated using a weighted mean of the average diffusion coefficients for pure sucrose and pure starch. Although the diffusion coefficients for amorphous and crystalline sucrose are quite different, this has a minor effect on the calculated diffusion coefficients for the range of crystallinities observed in the sucrose:starch mixtures. © 2001 Elsevier Science Ltd. All rights reserved.

*Keywords:* NMR imaging; Diffusion; STRAFI

### 1. Introduction

The transport of water in food materials is of general importance; it plays a part in processes such as cooking, drying, microbial spoilage and changes in quality of a range of food products during storage. Starch and sucrose:starch mixtures are model systems that should capture the essential physics of the ingress of water into a range of materials. The philosophy of this work is that studying the individual food components will lead to a better understanding of more complex composite systems.

It has been recognised for a number of years that starch, as a polysaccharide, can be treated in much the same way as a synthetic polymer and that, in particular, ideas such as glass transition can be successfully applied to starch and other food polymers [1]. This has implications for the diffusion of penetrants in starch. Diffusion effects can be characterised by a time exponent. In classical Fickian systems this time exponent is 1/2, i.e. the underlying diffusion effects exhibit a linear dependence on the square root of time. A frequently observed phenomenon in synthetic polymers is the so-called Case II diffusion [2,3]. In Case II diffusion a

time exponent of unity is observed. In practice, a continuum of exponents are found of which Fickian and Case II diffusion are simply the two more common limiting cases. There have been numerous models of Case II diffusion in polymers, the most successful of which are based on the physical model of Thomas and Windle [4]. The key point of the Thomas–Windle model is that the viscoelastic properties of the polymer matrix are important and that the penetrant molecule plasticises the polymer, changing the viscoelastic properties during the course of ingress. It is the coupling of the usual diffusion processes and the viscoelastic effects which leads to the observed time exponent of unity. Previous work by us indicated that Fickian diffusion is observed for the ingress of water vapour into amylose pellets and Case II diffusion is observed for the ingress of liquid water into amylose pellets [5]. The work presented here is an expansion of this initial investigation. It includes the effects of temperature and a two-phase mixture. In addition, the experimental method and sample preparation have been improved. The sucrose:starch system was chosen for two reasons: firstly it clearly has direct parallels with a range of food products and secondly it can be seen as being representative of a group of systems where one component is soluble and the other insoluble.

In this work transport properties are determined by

\* Corresponding author. Fax: +44-1223-337-000.

E-mail address: ian.hopkinson@phy.cam.ac.uk (I. Hopkinson).

examining the time evolution of a water content profile in an initially dry sheet to which water is supplied at one surface. This is done using stray field nuclear magnetic resonance imaging (STRAFI) [6,7], discussed in more detail below. Earlier work on the transport of water in starch was carried out almost exclusively using gravimetric methods [8,9] although there have been measurements by NMR relaxation methods of the self-diffusion coefficients of water in both starch [10,11] and sucrose [12]. The water content profile method has a number of advantages over the gravimetric methods: (a) it is less reliant on a model to analyse the data; (b) in principle it allows the determination of the mutual diffusion coefficient over a range of water contents in a single relatively brief experiment; and (c) it is straightforward to study the ingress of liquid water rather than water vapour and the investigation of soluble materials is also possible. Imaging studies are complementary to NMR relaxation measurements since they probe the mutual diffusion coefficient rather than the self-diffusion coefficient. The particular imaging method used here is especially sensitive at low water contents. The distinction between the mutual diffusion coefficient and the self-diffusion coefficient is that the mutual diffusion coefficient is measured in a non-uniform environment, in which the water content varies from point to point, whereas the self-diffusion coefficient is measured in a uniform environment and should be thought of as a mobility. Self-diffusion and mutual diffusion coefficients are linked via the sorption isotherm [11,13].

In a range of commonly found situations it is not pure water that penetrates starch but rather some solution containing a range of components. In particular, at sub-zero temperatures liquid water is available in the form of freeze concentrated solutions. Here we choose to study the broad effect of these solutes by studying the effect of changing the water activity of the penetrant solution. Indeed, in order to study the ingress of liquid water down to  $-20^{\circ}\text{C}$ , it is essential to use a lower-activity solution since freezing otherwise occurs, dramatically limiting the supply of liquid water.

Conventional nuclear magnetic resonance imaging, using switched field gradients, has been used to study the ingress of water into pasta [14] and wheat grains [15]. The drawback of this method is that it is difficult to image systems with short spin–spin relaxation times ( $T_2$ ), including solid materials and penetrants at low concentrations. This difficulty arises because maintaining resolution in short  $T_2$  systems requires that high field gradients be applied for short times and switched correspondingly quickly. The conventional MRI of short  $T_2$  systems therefore poses serious technical challenges. For this work we use STRAFI which has been developed in the last few years following the original work of Samoilenko et al. [7]. This technique has been specifically developed for high spatial resolution imaging of short  $T_2$  systems. The basis of STRAFI is to place the sample of interest in a high, linear field gradient, such as is found surrounding a high-field magnet. A broad

band radio frequency pulse is used to excite a thin slice of the sample, typically  $7\text{--}70\ \mu\text{m}$ , depending on the pulse length and the gradient strength. There are two methods for obtaining a ‘composition’ profile using STRAFI. The first method is to move the sample within the field gradient to excite successive slices and so build up a one-dimensional profile in the gradient direction. This is often described as the ‘sample sweep’ method and was used in our previous work and is described in detail by Benson and McDonald [16]. The second method is to keep the sample stationary while changing the frequency of the excitation pulse (frequency sweep). Again a one-dimensional profile of the sample is generated. It is this frequency sweep method which is used in this work and described in detail by Glover et al. [17]. The sample sweep method sets no restriction on the size of the sample in the direction of the profile ( $z$ -axis). However, the sample must fit within the excitation coil. In our implementation the sample is restricted to approximately 7 mm diameter in the  $x$ – $y$  plane. Previous experiments have found that ingress of the penetrant through the sides of the sample can occur. The frequency sweep method restricts the sample thickness to around 1 mm because it uses a surface coil upon which the sample is placed. However, this means that there is no size restriction in the  $x$ – $y$  plane and since only the centre of the sample in the  $x$ – $y$  plane is probed, it is free from the problems of side ingress. The drawback of the STRAFI method is that it is a high-bandwidth experiment and thus sacrifices the signal to noise ratio of the data considerably when compared with the conventional liquid state, long  $T_2$ , experiments.

## 2. Experimental

### 2.1. Sample preparation and characterisation

In this work we use waxy maize starch which is substantially composed of amylopectin and, henceforth, we will simply refer to waxy maize starch as ‘starch’. Starch and starch:sucrose mixtures, with around 30% added water, were extruded through a rectangular slot die using a twin screw extruder. This produced flexible ribbons of material with a dry weight basis water content of approximately 25%. Samples with dry mass fractions of starch of 100, 70 and 50% were prepared, with sucrose as the other main component. The extruded ribbons were subsequently compressed with a pressure of 10–15 MPa at  $100^{\circ}\text{C}$  against spacers to produce pressed sheets that were around 0.75 mm thick. The still flexible pressed sheets were then cut into 25 mm squares and dried, under a heavy metal disk, such that they remained flat. The 100 and 70% starch samples were dried overnight under vacuum at  $80^{\circ}\text{C}$ . After drying, the samples were stored over silica gel. The water content for samples stored in this way was found to be around 3%. This was determined by drying the samples under vacuum at

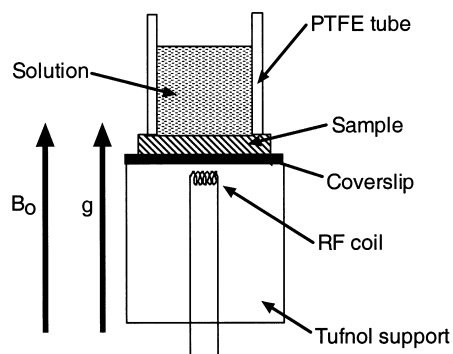


Fig. 1. Schematic diagram of the STRAFI experiment in 'frequency sweep' mode; the arrow indicated by  $B$  is the direction of the magnetic field and  $g$  indicates the gradient in the magnetic field.

80°C, without the weights used to maintain planarity, until there was no further mass loss.

Initially, the 50% starch samples were dried in the same way as the 70 and 100% starch samples. However, it was apparent by visual inspection that this resulted in samples where a sizeable fraction of the sucrose had crystallised. Subsequently, the pressed 50% starch samples were dried at room temperature under vacuum and only after several days were they heated to 80°C. This resulted in samples with a lower apparent crystallinity. A more quantitative determination of the crystallinity is described below.

Two more pure sucrose samples were prepared for the STRAFI experiments. The first was prepared by mixing a minimal amount of water with sucrose crystals and then pressing at 10–15 MPa at 100°C to produce a highly crystalline sample. The second was prepared by melting sucrose at approximately 200°C and then pouring the resulting melt into a cold metal mould to produce a substantially amorphous sample.

In order to characterise the sucrose crystallinity in the samples, differential scanning calorimetry (DSC) was performed using a Perkin–Elmer DSC 7. Thermograms were collected using a heating rate of 10°C min<sup>-1</sup>. Thermograms of pure crystalline sucrose exhibited a melting endotherm at 192.7°C (with  $\Delta H = 120.9 \text{ J g}^{-1}$ ). Amorphous samples prepared by quenching a molten sucrose sample in the DSC at 50°C min<sup>-1</sup> exhibited a glass transition at around 53.1°C with  $\Delta C_p = 0.46 \text{ J g}^{-1} \text{ K}^{-1}$ . The sucrose samples prepared for the STRAFI experiments were found to have mass fraction crystallinities of 16% for the amorphous sample and 86% for the crystalline sample, based on the size of the melting endotherm relative to that of the pure crystalline sample. In the case of the amorphous sample it was possible to confirm this value by measuring the amorphous fraction using the amplitude of the glass transition. The 70% starch samples exhibited no melting endotherms and so it was assumed that the sucrose was amorphous. The 50% starch samples exhibited melting endotherms, indicating crystallinities in the range 4–20% of the total sample mass.

## 2.2. NMR methods

STRAFI experiments were carried out using the 'frequency sweep' method described fully by Glover et al. [17]. As discussed previously, in this method the sample is placed in a large field gradient and successive slices of the sample are probed by varying the pulse frequency. In this work a 9.4 T superconducting solenoid magnet is used, producing a field gradient of 58 T m<sup>-1</sup> in the fringe field. The proton resonant frequency at the point of optimum gradient is around 235 MHz. The field gradient produces a change in resonant frequency of around 2.3 MHz mm<sup>-1</sup>. Data is acquired using a surface coil, upon which the sample is placed. This is illustrated in Fig. 1. The samples used here are thin sheets of the starch or sucrose:starch mixtures glued, on the underside, to glass coverslips. A PTFE tube is glued to the top of the sample. The PTFE tube is used as a well into which the solution for ingress is placed.

In these experiments the water content of the sample, as a function of position, is measured by probing the sample with the pulse sequence:  $\alpha_x - \tau - (\alpha_y - \tau - \text{echo} - \tau)_n$ , where  $\alpha_{x/y}$  is a radio frequency excitation pulse of flip angle  $\alpha$  and phase  $x/y$ .  $\alpha_{x/y}$  is nominally 90°,  $\tau$  is 30  $\mu\text{s}$  and  $n$  is 8. The pulse frequency is varied and this provides the spatial sensitivity. The frequency was increased by 66 kHz between successive applications of the pulse sequence corresponding to a spatial interval of 26  $\mu\text{m}$ . For each set of acquisition parameters, data from a uniform rubber phantom is also acquired and subsequently used to normalise data to correct for the loss of sensitivity as a function of distance from the surface coil. In principle, the echo signal amplitudes acquired for each slice give the spin–spin relaxation behaviour of that slice. The signal contains contributions, decaying exponentially in time, from various populations of protons within the system. Ideally, we would fit the data with a series of exponentials, each characterised by a decay time and an amplitude, then identify the relaxation corresponding to water and use the amplitude of that decay as a measure of the water content. However, since we only collect eight echoes with relatively poor signal to noise, this scheme is impractical. Instead, the intensities of the echoes are summed up and the water content is determined from an empirical calibration curve. To construct the calibration curve it is necessary to prepare samples with a range of uniform water contents. It was found that this was possible for the 100% starch samples. However, for the sucrose containing samples it was not possible to prepare a range of water contents. Therefore, just the 100% starch samples with different, uniform water contents were measured using STRAFI at 20°C. The results of these calibration experiments are shown in Fig. 2. The calibration data of the summed echo intensity versus water content were fitted with a straight line and in the remainder of this work water concentrations in the 100% starch samples will be calculated from this fit. The calibration curve does show some deviation from linearity at low water contents. This is because glass transition occurs in

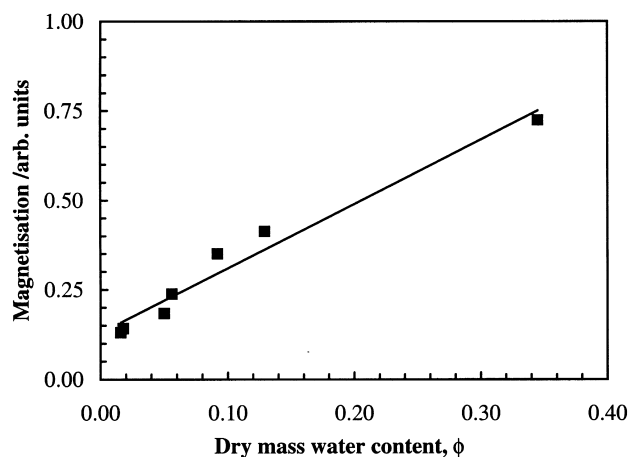


Fig. 2. Calibration curve for the summed echo intensity versus water content for 100% starch. The line is a linear fit to the data.

these samples at around 20°C for a water content of around 0.1. The consequent increase in the spin–spin relaxation time causes an increase in signal intensity in the later echoes. We should also note that this calibration is only strictly applicable at 20°C.

In this work three experimental variables are considered in the ingress properties of water into starch mixtures. These are temperature, water activity  $a_w$  and sucrose content in the starch plaque. As a preliminary to the measurement of water ingress profiles some gravimetric experiments were carried out. The 100% starch samples, prepared in the same manner as for the STRAFI experiments, were immersed in a range of solutions of different water activity, and their weight measured at intervals — taking care to remove the surface liquid. Two types of solution were used to control water activity: saturated salt solutions [18] and water:glycerol mixtures [19]. In all the cases the activity of the solution was measured by measuring the relative humidity of the equilibrated water vapour above the solutions using an electronic meter. The following saturated salt solutions were used: KAc ( $a_w = 0.205$ ),  $MgCl_2$  ( $a_w = 0.335$ ),  $Ca(NO_3)_2$  ( $a_w = 0.555$ ), and NaCl ( $a_w = 0.76$ ). The samples were kept at a constant temperature of 25°C. Vapour uptake experiments, where the mass increase of samples in vapour above the solutions was measured, were also carried out. The results of these experiments will be discussed more fully below. In short, it was found that the sorption from saturated salt solutions exhibited strong specific ion effects; therefore, glycerol:water solutions and sucrose solutions were used for subsequent experiments.

STRAFI experiments were used to follow the ingress of water in the following systems:

1.  $a_w = 0.8$  glycerol:water mixture into 100% starch;
2. 25% sucrose solution into 100% starch;
3. 25% sucrose solution into 70% starch;
4. 25% sucrose solution into 50% starch;

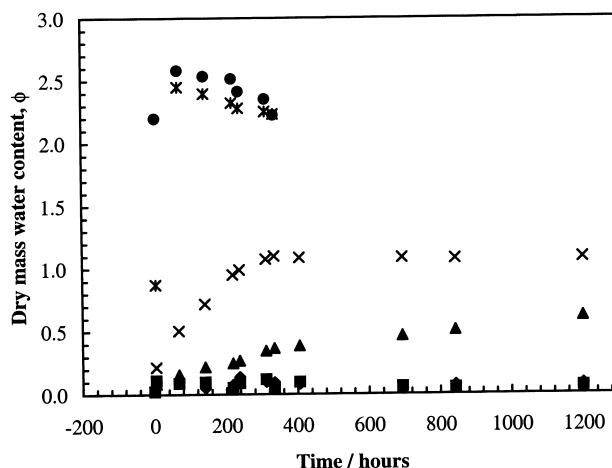


Fig. 3. Sorption kinetics for the uptake of water from glycerol:water mixtures:  $a_w = 0.0$  (filled diamond),  $a_w = 0.225$  (filled square),  $a_w = 0.425$  (filled triangle),  $a_w = 0.585$  (cross),  $a_w = 0.74$  (star) and  $a_w = 1.0$  (filled circle).

5. 25% sucrose solution into amorphous and crystalline sucrose (20°C only);
6. various  $a_w$  solutions into 100% starch (20°C only).

For experiments (1)–(4) temperature was used as a variable. The activity of the equilibrium water vapour above a 25% sucrose solution was found to be 0.93.

Temperature was controlled using a stream of dried air, the temperature of which was maintained using electrical heating. Sub-ambient temperatures were achieved by first cooling the gas with either dry ice or liquid nitrogen. In this way, the temperature of the sample was varied between  $-20$  and  $45^\circ\text{C}$  with a precision of around  $0.5^\circ\text{C}$ . For samples at higher temperatures a continuous series of water content profiles were acquired at approximately 5 min intervals for periods of up to 2 h. At lower temperatures, typically below  $0^\circ\text{C}$ , the rate of ingress was much slower and so the data were obtained over a period of up to 1 week with profiles measured at intervals of the order of days and the sample stored at the appropriate temperature between measurements.

### 3. Results

#### 3.1. Gravimetric experiments

We started by looking at the results of the gravimetric uptake experiments. Uptake was monitored until mass increase had ceased or until the sample in question had disintegrated. Fig. 3 shows the kinetics of uptake for the glycerol:water mixtures into 100% starch. The samples exposed to high water activity reach equilibrium in a matter of tens of hours while those with the lowest activity show no discernable uptake of water even after 50 days. Following a large initial uptake of water, the samples in the highest

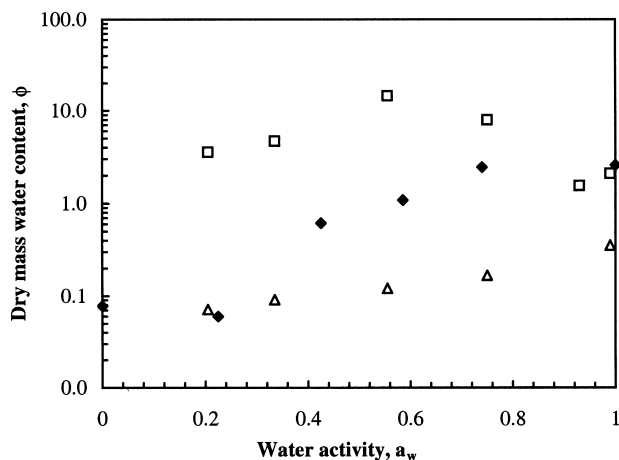


Fig. 4. Sorption isotherms for 100% starch in direct contact with glycerol:water mixtures (filled diamond) or saturated salt solutions (open square), and starch in contact with vapour of specified activity (open triangle).

activity glycerol:water solutions exhibit a small reduction in mass uptake at later times. This is possibly due to the solubilisation, or even breakdown, of some fraction of the starch. Similar kinetic behaviour is seen for the uptake of the saturated salt solutions (not shown), with the lowest-activity solutions showing very low uptake rates. Equilibrium was achieved for the samples exposed to vapour and to the glycerol:water liquid sorption experiments, excluding the  $a_w = 0.425$  glycerol water mixture. Among the saturated salt solutions, only the NaCl solution,  $a_w = 0.76$ , appeared to reach equilibrium.

Fig. 4 shows the final mass uptake for the three sets of experiments. The data are shown on a log scale for clarity. For both glycerol:water and saturated salt solutions it was found that the mass of water adsorbed from the liquid in direct contact was greater than that adsorbed from the vapour of the same water activity. For the glycerol:water ingress the difference between the final mass uptake for the liquid contact and for the vapour contact increased with activity. It was found that for the samples immersed in saturated salt solutions the final adsorbed mass was much higher than for the glycerol:water mixtures, with the samples adsorbing up to 15 times their original weight of water. For these samples the increased water uptake was not monotonic with water activity. This effect was particularly marked for  $\text{Ca}(\text{NO}_3)_2$ .

### 3.2. Ingress experiments

STRAFI of the ingress of water into samples was carried out to times that were short in comparison with the time required for the samples to reach an equilibrium water content. Fig. 5 shows a representative diffusion profile for the uptake of water of activity 0.8 into a pure starch. The original sample surface is located at 0 on the depth axis, as determined from a profile of the sample before the penetrant

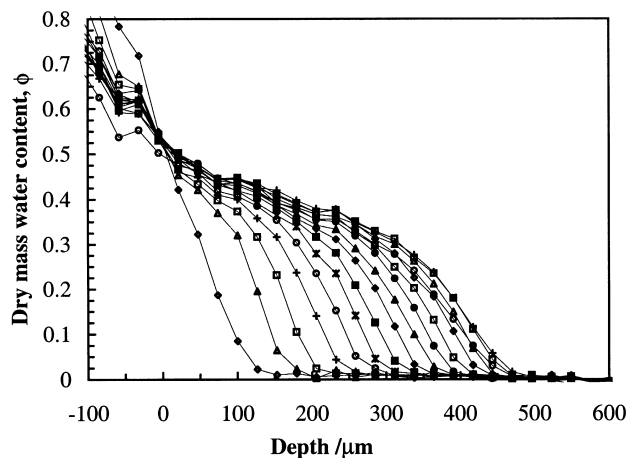


Fig. 5. Water content profiles for the ingress of 25% sucrose solution into 0:100 starch at 0°C; ingress is from the left and the time between profiles is 6 min.

is added. The ingress is from the left into an initially dry sample. The time between profiles is 6 min. During ingress, the sample swells. This is illustrated by the reduction in water content, as ingress proceeds, for positions to the left of the original sample surface. The shape of the profiles indicates that the diffusion process does not arise from a mutual diffusion coefficient which is fixed with respect to the water content. If this were the case, then the profiles would be described by an error function, which is concave. Profile shapes for the ingress of water into pure sucrose, 70% starch and 50% starch were qualitatively different from those for ingress into 100% starch. They exhibited ingress fronts which were sharper, i.e. the water content increased more abruptly as a function of position. Qualitatively, it was observed that the ingress was most rapid for the pure sucrose samples and that the rate of ingress decreased in the order 50, 70 and 100% starch at a fixed temperature. As the temperature decreased, the ingress becomes markedly slower. The profile shape for the ingress of 25% sucrose solution was different below 0°C, temperatures at which the solution undergoes substantial freezing. Ingress profiles at  $-10^\circ\text{C}$  are shown in Fig. 6. In these samples the water content does not increase immediately to a constant value which is maintained throughout the experiment, as is the case at higher temperatures.

## 4. Discussion

### 4.1. Gravimetric experiments

The slower ingress at lower water activity can be explained by a diffusion coefficient which varies with the water content. Samples immersed in liquid absorbed far more water than those exposed to vapour of the same activity. This can be attributed to the fact that the starch immersed in water will form a two-phase system. One is a starch-rich phase and the other is a water-rich phase of the

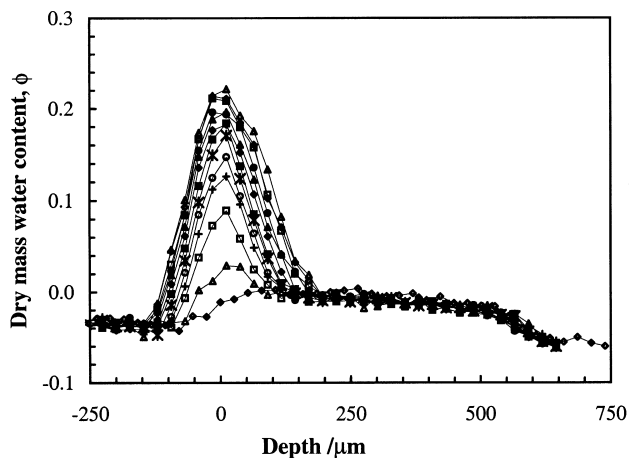


Fig. 6. Water content profiles for the ingress of 25% sucrose solution into 0:100 starch at  $-10^{\circ}\text{C}$ ; ingress is from the left and the profiles are taken at 52 min intervals. The height of the 'peak' in water content increases with time.

same activity. The amount of the water-rich phase is not controlled since the samples are immersed in an excess of solution and so the amount of water taken up by the sample will depend on the volume of 'pores' which open up in the sample. Therefore, uptake is limited by the mechanical stability of the starch — how much it can be swollen before it disintegrates. The effect is much greater in the saturated salt solutions. This is most likely due to specific ion interactions which change the structure of the starch, allowing a larger pore volume to form.

#### 4.2. STRAFI experiments

The STRAFI experiments produced a large number of water content profiles. In order to test whether or not the observed profiles are due to Fickian diffusion, we plot the diffusing front position as a function of  $\sqrt{t}$ , where  $t$  is the time. In the case of Fickian diffusion, such a plot will appear linear so long as the front does not approach the far end of the sample. We define the front position as the position where the front reaches half the maximum concentration. The front position is measured relative to the original sample surface whose position is established from a profile measured before the ingress solution is added. Fig. 7 shows the front positions as a function of  $\sqrt{t}$  for a selection of ingress experiments. The data are all well approximated with linear fits, indicating that Fickian diffusion is taking place. Fickian diffusion was found for all the samples, i.e. for pure starch, pure sucrose and the mixtures. We can obtain a 'characteristic' diffusion coefficient  $D_{av}$  from these plots since we know that the characteristic diffusion length is given by  $(D_{av}t)^{1/2}$  which can be equated to the front position.  $D_{av}$  is simply the slope of the front position versus the  $t^{1/2}$  plot. This measure will be used frequently in the subsequent discussion since it is a robust and straightforward way of parametrizing the profile position data

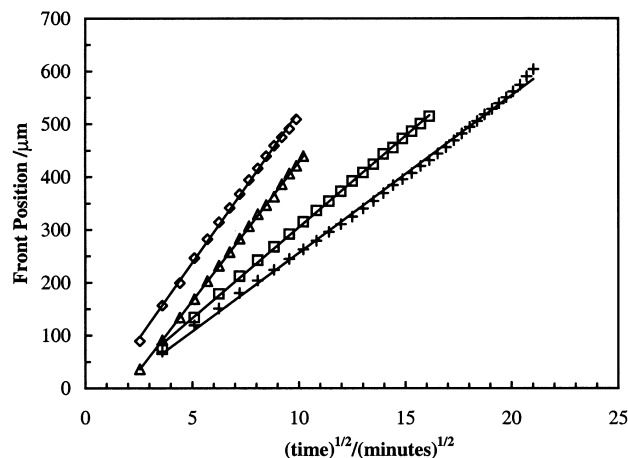


Fig. 7. Front positions versus  $(\text{time})^{1/2}$  for the ingress of 25% sucrose solution into 70% starch at  $20^{\circ}\text{C}$  (open diamonds),  $10^{\circ}\text{C}$  (open triangles),  $0^{\circ}\text{C}$  (open squares), and  $-5^{\circ}\text{C}$  (crosses). Solid lines are linear least squares fits to the data.

and is related to the magnitude of the mutual diffusion coefficient.

The average diffusion coefficient for the ingress of 25% sucrose solution into 100% starch at  $20^{\circ}\text{C}$  was found to be  $2.49(4) \times 10^{-11} \text{ m}^2 \text{ s}^{-1}$ . This compares with the average diffusion coefficients into crystalline and amorphous sucrose samples of  $5.04(8) \times 10^{-11}$  and  $11.7(2) \times 10^{-11} \text{ m}^2 \text{ s}^{-1}$ , respectively. This mutual diffusion coefficient is comparable in magnitude to the self-diffusion coefficients measured by Girlich et al. [12] using NMR relaxation methods for a range of sucrose:water mixtures. These diffusion coefficients for sucrose actually relate to a mobility in a composite material since the crystalline sample is 86% crystalline and therefore 14% amorphous and the amorphous sample is 15% crystalline. We will discuss diffusion in composite materials below. Sucrose and starch have essentially the same chemical composition. Therefore, the differences in the diffusion coefficients must be due to physical effects. A likely reason is a difference in the mechanical relaxation times. During ingress, the penetrant will attempt to swell the substrate. The rate of transport through the sample will depend to a degree on how easily the sample can be swollen. In previous work, we found that the ingress of water into amylose was described by Case II transport. Case II transport occurs when the characteristic times for relaxation and diffusion are comparable. The difference here is that an amylopectin-rich starch is used instead of amylose and the samples produced are structurally more rigid. This has the effect of increasing the mechanical relaxation time while the diffusional relaxation time remains approximately the same and so the system moves away from Case II behaviour. The observed ingress rate in starch is thus limited by the reluctance of the starch to swell to accommodate the water. In pure sucrose this is not a limitation because sucrose dissolves easily (i.e. relaxes rapidly).

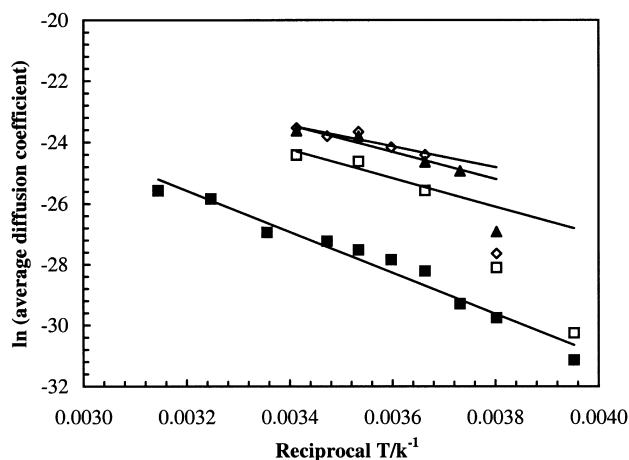


Fig. 8. Arrhenius style plot of  $\ln D$  versus reciprocal temperature. 25% sucrose into 50% starch (open diamond), 70% starch (filled triangle) and 100% starch (open square) and ingress of  $a_w = 0.8$  glycerol:water into 100% starch (filled square).

#### 4.3. Temperature dependence

If we assume that the temperature dependence of the average diffusion coefficient  $D(T)$  is controlled by an energy barrier, then it should obey an Arrhenius expression of the form:

$$D(T) = D_0 \exp(-\Delta H/RT) \quad (1)$$

where  $\Delta H$  is the activation energy,  $D_0$  a constant prefactor,  $R$  the gas constant and  $T$  the temperature. A plot of  $\ln D_{av}$  versus  $1/T$  will be linear. Such a plot is shown in Fig. 8. It clearly shows that the ingress of 0.8 activity water into starch obeys an Arrhenius law. The ingress of 25% sucrose at higher temperatures is also described by an Arrhenius law. However, for lower temperatures the 25% sucrose data deviates from the linear trend seen at higher temperatures. The physical explanation for this is that at  $-10$  and  $-20^\circ\text{C}$  a significant proportion of the sucrose solution freezes and the remaining liquid has a lower activity. Therefore, the rate of ingress is reduced by the reduction in the available water and the reduced activity of the water. The effect of the reduced availability of water can be seen in Fig. 6 which shows the ingress of 25% sucrose solution into 100% starch at  $-10^\circ\text{C}$ . At this temperature the sucrose solution is mainly frozen but some freeze concentrated liquid remains. The profiles clearly show that the water content at the surface increases with time in contrast to the data collected at  $0^\circ\text{C}$  where the surface water content is constant. This means that at low temperatures the water supply is a limiting step. The flux of water from the frozen phase is most likely to depend on the detail of the microstructure of the frozen solution. We have made no attempt to investigate this behaviour further.

The values for the activation energy  $\Delta H$  were obtained by making linear fits to the  $\ln D_{av}$  versus  $1/T$  plots, excluding the sub-zero data for 25% sucrose because the water supply

Table 1  
Activation energies for the ingress of water into starch

Sample	Activation energy $E_A$ ( $\text{kJ mol}^{-1}$ )
50% starch, ingress of 25% sucrose	$28 \pm 7$
70% starch, ingress of 25% sucrose	$36 \pm 6$
100% starch, ingress of 25% sucrose	$39 \pm 13$
100% starch, ingress of $a_w = 0.8$	$56 \pm 4$

limit described above indicates a change of mechanism and so the data are not consistent with those collected above  $0^\circ\text{C}$ . The results of these fits are shown in Table 1. The data show that the activation energy is only weakly dependent on the composition and is lower for the ingress of 25% sucrose than for the lower-activity glycerol:water solution. These data can be compared with the gravimetric results of Fish [9], who found the results shown in Table 2. These data are ordered in terms of the average water content of the sample for the period during which the diffusion coefficient was measured. The results are for the samples in water vapour and are the same for sorption and desorption. The best comparison with the Fish data is the data with the lowest average water content (0.8%) since the ingress observed is into an initially 'dry' sample with around 2% initial water content. In this limit, the activation energy is  $41 \text{ kJ mol}^{-1}$ , which fits in well with our data. We can find an activation energy from Girlich's data for a 70 w/w% sucrose solution which turns out to be  $33 \text{ kJ mol}^{-1}$ . Such a value would be consistent with an activation energy that varied only slightly with the sucrose content, as suggested above.

#### 4.4. Composition dependence

We now go on to look at how the average diffusion coefficient  $D_{av}$  in the pure materials relates to the diffusion coefficient in the 50 and 70% starch mixtures and also whether an effect of sucrose crystallinity can be seen. Table 3 summarises the average diffusion coefficient values obtained for the ingress of 25% sucrose solution at  $20^\circ\text{C}$ . On inspection, it would appear that the  $D_{av}$  for the 50% starch sample lies somewhere midway between the values for 100% starch and amorphous sucrose, so our first step is to attempt to predict the values of  $D_{av}$  by weighted arithmetic means of the values for the pure components. The results of this analysis are shown in Table 3. For the pure

Table 2  
Activation energies for the ingress of water into starch from Fish [9]

Water content (w/w%)	Activation energy $E_A$ ( $\text{kJ mol}^{-1}$ )
0.8	41.0
6.3	33.9
14.1	26.4
80	18.8

Table 3

Measured and predicted values for the average diffusion coefficient (in  $\text{m}^2 \text{s}^{-1}$ ) for the ingress of 25% sucrose solutions at 20°C. For the 50% starch samples the percentage figure indicates the overall crystallinity of the sample arising from the sucrose

	$D \times 10^{11} (\text{m}^2 \text{s}^{-1})$	
	Measured	Predicted
Pure starch	2.49(4)	
Crystalline sucrose	5.04(8)	3.7(1)
Amorphous sucrose	11.7(2)	13.2(4)
50% starch 4%	6.74(8)	7.5(4)
15%	5.0(3)	6.4(4)
21.4%	6.74(2)	5.8(4)
Mean	6(1)	6.6(9)
70% starch	5.5(1)	5.7(4)

sucrose samples we have measured the crystalline and amorphous fractions, so we can make a prediction for the  $D_{\text{av}}$  for 100% amorphous and 100% crystalline sucrose. The predictions for these systems are shown in the second column.

For the remaining samples we calculate the average values based on these 100% amorphous and crystalline predictions. It is difficult to discern a trend in the diffusion values for the three 50% starch samples with different crystallinity. However, the average value obtained for the three samples is consistent with the prediction, as is the predicted value for the 70% mixture.

Crank [20] reports a model by Tsao, further developed by Cheng and Vachon, for predicting the diffusion coefficient in a heterogeneous medium. They assume a random distribution of irregular particles and calculate the diffusivity of the ensemble by representing these particles as a series of parallel sheets. Diffusion coefficients can be calculated for this ensemble. To do this both Tsao, and Cheng and Vachon make assumptions about the distribution of the dispersed phase. Cheng and Vachon make sufficient assumptions that only the dispersed phase volume fraction is required to estimate the diffusion coefficient. We have found that the results of these models are essentially the same as those found here, so long as it is assumed that the starch forms the continuous phase. This suggests that our empirical scheme is simply an approximation to a more physical model.

Since it has been established that the ingress of the liquid is Fickian, it is possible to obtain  $D(\phi)$  analytically using the change of variable  $z \Rightarrow zt^{-1/2}$ , known as the Boltzmann transform, in which case:

$$D(\phi) = -\frac{1}{2} \left[ \frac{\partial \xi}{\partial \phi'} \right]_{\phi} \int_0^{\phi} \xi d\phi' \quad (2)$$

where  $\xi = zt^{-1/2}$ , subject to transformable boundary conditions. In the common case where  $\phi(0)$  is constant with time,

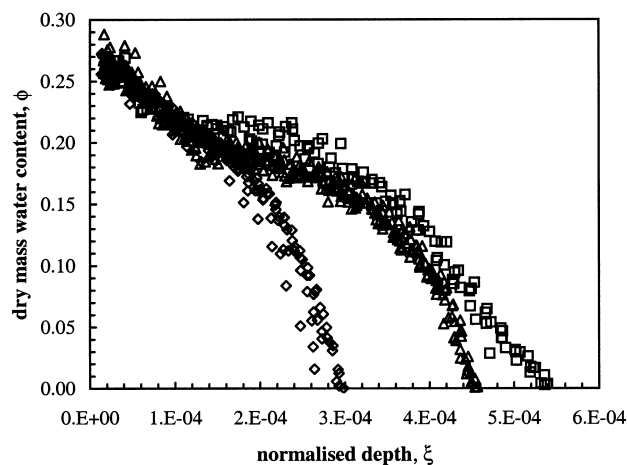


Fig. 9. Profiles normalised following the Boltzmann scheme from the ingress of 25% sucrose solution into 100% starch at 0°C (open diamond), 10°C (open triangle) and 20°C (open square).

it is possible to superimpose diffusion profiles collected at different times by the use of this transform. We found that for the ingress into pure starch samples it was possible to apply the Boltzmann transform to produce profiles that superposed well. This is shown in Fig. 9. For the sucrose containing samples it was not possible to superpose profiles using the Boltzmann transform. This is because in these samples the water 'front' is sharp and therefore there are at most two or three points between the lowest water contents and the highest water contents. For the ingress of sucrose solution into starch the Boltzmann transformed ingress profiles superpose for the three temperatures above the freezing point of the sucrose solution at water contents above 0.2. This suggests that the starch-rich phase of the sample has a water content of around 0.2. Above this level, water occurs in liquid form and as such the transport rate is much less dependent on temperature. This phase behaviour would be in agreement with the observed isotherm data, which shows a water content for starch equilibrated with the saturated vapour above a sucrose solution of around 0.2. Fig. 10 shows the mutual diffusion coefficient as a function of water content, obtained from polynomial fits to the normalised profiles shown in Fig. 9. In our previous paper, we found that the calculation of the mutual diffusion coefficient was prone to numerical error. A 15% uncertainty in the mutual diffusion coefficient at any particular water content is indicated by this work and shown in Fig. 10. It is this uncertainty in the mutual diffusion coefficient that leads to the apparent decrease in the mutual diffusion coefficient, at some water contents, as the temperature is increased. Such a decrease is inconsistent with the average diffusion coefficients and with expectations of the variation of the diffusion coefficient with temperature.

As a final piece of analysis, we compare the values of  $D_{\text{av}}$  obtained using different solutions to the mutual diffusion coefficient calculated using the Boltzmann transform for



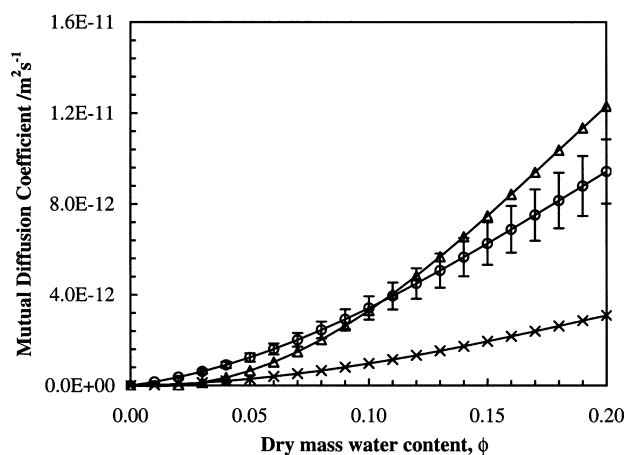


Fig. 10. Mutual diffusion coefficient obtained by the Boltzmann transform for the ingress of 25% sucrose solution into starch at 0°C (cross), 10°C (open triangle) and 20°C (open circle). Error bars show an estimated error of 15%.

the ingress of water into starch. These data are plotted as a function of the water activity obtained from a fit to the sorption isotherm. The results of these calculations are shown in Fig. 11. They show that at higher activities there is fair agreement between  $D_{av}$  and the mutual diffusion. At lower activities the measured  $D_{av}$  are an order of magnitude smaller than the mutual diffusion coefficient. The discrepancy probably arises from a systematic error in the conversion of arbitrary magnetisation units to water content at low water content. This effects the shape of the  $\xi(\phi)$  curve, which is used to calculate the  $D(\phi)$ . In the low  $\phi$  region of the curve we are also more prone to numerical error since the slope  $d\xi/d\phi$  is smaller than at higher  $\phi$  and the integration range is small. Measurements on simulated profiles show that the error is not due to the slightly differing definitions of  $D_{av}$  and  $D(\phi)$ .

## 5. Conclusions

We have shown how stray field NMR imaging can be utilised to analyse the ingress of water into starch and starch:sucrose mixtures and we have analysed how this behaviour varies with temperature and water activity. We have found that the temperature dependence of the diffusion coefficient can be described by an Arrhenius type expression and that the activation energy so derived appears to vary only slightly with the sucrose content. The average diffusion coefficients  $D_{av}$  obtained for sucrose:starch mixtures can be estimated from the mass weighted arithmetic mean of the  $D_{av}$  for pure starch and sucrose.

## Acknowledgements

We are grateful to Baltasar Valles-Pamies (University of Nottingham, Department of Food Science) for sample

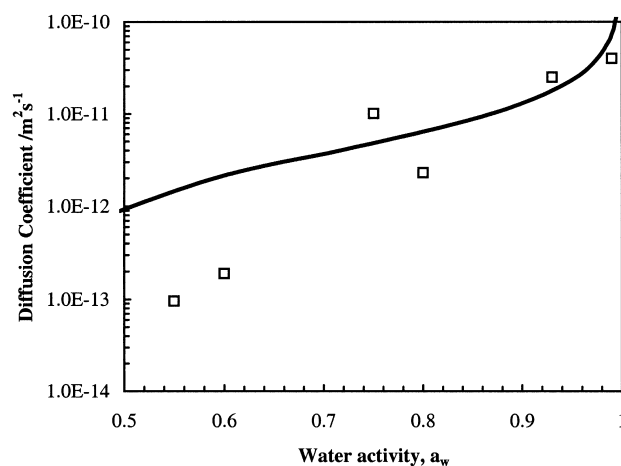


Fig. 11.  $D(a_w)$  versus  $a_w$ , where  $a_w$  is the activity of the water undergoing ingress, the solid line is the mutual diffusion coefficient,  $D(\phi)$  is calculated using the Boltzmann transform, and the open squares are values of  $D_{av}$  measured from the experimental ingress data for solutions of different  $a_w$ .

preparation and I.H. is grateful to Nestlé for funding. We would like to thank the EPSRC for funding the STRAFI facility at the University of Surrey.

## References

- [1] Blanshard JMV, Lillford PJ. The glassy state in foods. 1st ed., vol. 1. Nottingham, UK: Nottingham University Press, 1993.
- [2] Hui C-Y, Wu K-C, Lasky RC, Kramer EJ. Case-II diffusion in polymers. I. Transient swelling. *J Appl Phys* 1987;61(11):5129–36.
- [3] Hui C-Y, Wu K-C, Lasky RC, Kramer EJ. Case-II diffusion in polymers. II. Steady-state front motion. *J Appl Phys* 1987;61(11):5137–49.
- [4] Thomas NL, Windle AH. A theory of Case II diffusion. *Polymer* 1982;23:529–42.
- [5] Hopkinson I, Jones RAL, Black S, Lane DM, McDonald PJ. Fickian and Case II diffusion of water into amylose: a stray field NMR study. *Carbohydr Polym* 1997;34:39–47.
- [6] McDonald PJ. Stray field magnetic resonance imaging. *Prog NMR Spectrosc* 1997;30:69–99.
- [7] Samoilenko AA, Artemov DY, Sibel'dina LA. Formation of sensitive layer in experiments on NMR subsurface imaging of solids. *JETP Lett* 1988;47:417–9.
- [8] Luyben KCAM, Olieman JJ, Bruin S. Concentration dependent diffusion coefficients derived from experimental drying curves. In: Musumda AS, editor. *Drying '80*. New York: Hemisphere Publishing Corporation, 1980. p. 233–43.
- [9] Fish BP. Diffusion and equilibrium properties of water in starch. 1st ed., vol. 5. London: HMSO, 1957.
- [10] Ohtsuka A, Watanabe T, Suzuki T. Gel structure and water diffusion phenomena in starch gels studied by pulsed field gradient stimulated echo NMR. *Carbohydr Polym* 1994;25:95–100.
- [11] Kuhn K, Lechert H. Determination of Fickian diffusion coefficients of water in foods using nmr-techniques and the DARKEN-equation. *Lebensm-Wiss Technol* 1990;23:331–5.
- [12] Girlich D, Ludeman HD, Buttersack C, Buchholz K. c,T-dependence of the self diffusion in concentrated aqueous sucrose solutions. *Z Naturforsch, C* 1994;49c:258–64.
- [13] Duda JL, Ni YC, Vrentas JS. An equation relating self-diffusion and mutual diffusion coefficients in polymer-solvent systems. *Macromolecules* 1979;12(3):459–62.

- [14] Hills BP, Babonneau F, Quantin VM, Gaudet F, Belton PS. Radial NMR microimaging studies of the rehydration of extruded pasta. *J Food Engng* 1996;27:71–97.
- [15] Stapley A. Diffusion and reaction in wheat grains, PhD thesis, 1995, Cambridge.
- [16] Benson TB, McDonald PJ. Profile amplitude modulation in stray-field magnetic-resonance imaging. *J Magn Reson, Ser A* 1995; 112:17–23.
- [17] Glover PM, McDonald PJ, Newling B. Stray-field imaging of planar films using a novel surface coil. *J Magn Reson* 1997; 126:207–12.
- [18] Winston PW, Bates DH. Saturated solutions for the control of humidity in biological research. *Ecology* 1960;41(1):232–7.
- [19] Braun VJ, Braun JD. A simplified method of preparing solutions of glycerol and water for humidity control. *Corrosion* 1958;14(3): 117t–8t.
- [20] Crank J. *The mathematics of diffusion*, vol. 1. Oxford, UK: Oxford University Press, 1975.